THE ASTROPHYSICAL JOURNAL, 345:480–488, 1989 October 1

PHYSICAL REALISM IN THE ANALYSIS OF STELLAR MAGNETIC FIELDS. II. K DWARFS[1]

GEOFFREY W. MARCY
Department of Physics and Astronomy, San Francisco State University

AND

GIBOR BASRI
Astronomy Department, University of California, Berkeley
Received 1988 November 28; accepted 1989 March 25

ABSTRACT

We have carefully searched for Zeeman broadening in the absorption line profiles of 11 late G and K dwarfs. We analyze high signal-to-noise spectra in the near-infrared by solving the line transfer problem, including separate treatment of the Stokes parameters, in a full-model atmosphere. A line having low Zeeman sensitivity is used to determine the two unknown stellar parameters, Fe/H and macroturbulent velocity, which are then held fixed in the synthesis of a Zeeman-sensitive line. Comparison of the synthetic profile to that observed permits detection and measurement of Zeeman broadening. We have refined our original work with improved oscillator strengths and a disk integration treatment of velocity broadening.

Six of the 11 stars exhibit clear Zeeman broadening, the most extreme being ϵ Eri and ξ Boo A, having field strengths, B, and surface filling factors, f, of (1000 G, 30%) and (1600 G, 22%), respectively. The quantity Bf correlates with chromospheric Ca II emission and with stellar rotation. In the latter correlation, the residuals correlate with $T_{\rm eff}$, which suggests that magnetic fields increase with declining stellar mass as well as with rotation.

We find two stars, σ Dra and 54 Psc, that exhibit no Zeeman broadening at all, showing that magnetically weak stars definitely exist later than K0. Interestingly, 61 Cyg A is among the stars showing clear Zeeman broadening, contrary to expectations for an old, slow rotator. We find no field strengths that exceed 1600 G and no filling factors that exceed 30%, unlike previous studies in which field strengths up to 3000 G and filling factors over 50% were claimed.

Subject headings: stars: atmospheres — stars: late-type — stars: magnetic — Zeeman effect

I. INTRODUCTION

It is widely thought that the presence of chromospheric and coronal gas on G, K, and M main-sequence stars is related, as on the Sun, to surface magnetic fields. Support for this view has come from detections of the Zeeman effect in photospheric lines, as confirmed independently now by a number of groups, namely, Robinson, Worden, and Harvey (1980); Marcy (1984); Gray (1984); Saar (1988*a*); Basri and Marcy (1988, hereafter Paper I); and Mathys and Solanki (1988). These groups all find field strengths for G and K dwarfs in the range 1000–3000 G, and the fraction of the surface covered by fields is found to be substantial, often near 50% for the most chromospherically active stars. However, the magnetic field measurements for a particular star by different groups typically do not agree well enough to investigate the relevant stellar physics with confidence.

In principle, magnetic field measurements may be used to address two longstanding questions in stellar astrophysics: (1) What is the empirical dependence of the stellar chromospheres and coronae on surface magnetic fields and what is the underlying physics? (2) How are magnetic fields related to stellar rotation and convection, and what constraints may be placed on the underlying magnetic dynamo processes? The work of both Marcy (1984) and Saar (1988*b*) have demonstrated the existence of the dependences mentioned above, but accuracy in the quantitative dependence is lacking, primarily owing to the difficulty in the Zeeman analysis. Another difficulty in using the magnetic field measurements to understand either the heating rates of upper atmospheres or the efficiency of dynamo processes is that both depend on stellar mass, the former via differences in surface turbulence, and the latter via differences in convection zone characteristics.

Indeed, the magnetic field measurements to date suggest that the prevalence of strong fields increases with spectral type (Marcy 1984; Gray 1984), despite a generally declining rotation rate. For example, in a sample of 18 F, G, and K dwarfs, Gray (1984) detected Zeeman broadening in all those later than G6, but in almost none earlier. Indeed, one wonders whether a nonmagnetic K dwarf even exists. In particular, we noted in Paper I that HD 166620, a relatively quiet star chromospherically, nonetheless exhibited small Zeeman broadening. Similarly, 61 Cyg A was found to show Zeeman broadening (Marcy 1984) despite being chromospherically inactive (e.g., Simon and Fekel 1987). However, Saar and Linsky (1985) found no Zeeman splitting in infrared FTS spectra of 61 Cyg A (but also not for ϵ Eri, an active star).

We attempt to improve this situation in two ways. First, we implement an LTE line transfer analysis of Zeeman broadening that incorporates much of the known atmospheric physics, and, second, we adopt a stellar sample representing a narrow range in masses, namely, spectral type G8–K5. The paper is organized as follows. Section II describes the Zeeman analysis, especially the changes from Paper I. Section III contains the resulting magnetic fields for the 11 G and K dwarfs. Section IV*a* provides a discussion of the errors and a comparison with

[1] Research reported here is based on data collected at the Lick Observatory run by the University of California.

other measurements, and § IV*b* describes correlations of the magnetic fields with rotation, chromospheric activity, and stellar mass.

II. ANALYSIS

Most previous analyses of magnetic fields on cool stars have primarily used extensions of the Unno (1956) analysis with various levels of approximation. These analyses ignore some of the relevant physics, which perhaps can best be seen from the fact that observed profiles are subjected to an arbitrary scaling, and the line strength is characterized by a single parameter that is independent of atmospheric depth. In almost all cases, the collisional broadening of the line is accounted for in an artificial way. The latest refinement of these methods is by Saar (1988*a*). Most analyses have relied (as does ours) on the comparison of magnetically sensitive and insensitive lines to remove much of the unknown or untreated stellar physics differentially. The approach of Mathys and Solanki (1988) is somewhat different in that it attempts to do without any line transfer treatment and uses instead empirical scaling relations calibrated from solar work for a large number of lines. Such an approach is even more removed from physical analysis, although the authors intend to check their method against line transfer results.

In Paper I we introduced our new physical analysis technique for stellar magnetic fields, which includes computing the radiative transfer of all Stokes components through a model stellar atmosphere. In this paper we have introduced two improvements to that method. We adopt *gf*-values for the lines of interest based on the detailed laboratory work of Blackwell *et al.* (1982) rather than those of a semiempirical approach. In changing from the Kurucz and Peytremann (1975) values to those of Blackwell *et al.* (1982) (generally considered the best measurements to date), we introduce a small differential change in our Zeeman sensitive and insensitive lines, since the ratio between them is different in these two papers. For $\lambda 8468$, log *gf* changes from -2.24 to -2.07, and for $\lambda 7748$, the change is from -1.86 to -1.76. This is the major source of the change in fields derived here compared with those for stars in common in Paper I.

The other change is in our conversion from calculated specific intensity profiles at selected view angles to the synthetic flux profile. In Paper I we used a three-angle Gaussian quadrature scheme to convert to flux, and then convolved this with the rotational broadening function and Gaussian macroturbulent broadening function afterward. This can be criticized on several grounds: (1) the center-to-limb variation of the intensity profiles is correlated with rotational Doppler shift and is not treated with the convolution method, (2) the real macrobroadening mechanism is better represented by bulk flows on the stellar surface (not necessarily normally distributed) rather than by an ex post facto Gaussian process and, (3) the pattern of Zeeman components is a function of view angle to the magnetic field. Some of these points are discussed by Smith (1978) and Bruning (1984), who argue that a radial-tangential treatment (to approximate convective cells) with an explicit disk integration is superior. This procedure is, of course, also an ad hoc treatment of a more complex process. Dravins (1988) argues that if detailed granule models are studied, there is no need for any further velocity broadening. Nonetheless, it is not difficult to implement the disk integration scheme, and it definitely addresses points 1 and 3 above.

We combine the theoretical intensity profiles for eight different values of $\cos \theta$ in a disk-integration scheme to compute the synthetic flux profiles. Tests made with finer grids of $\cos \theta$ showed that eight values were sufficient to achieve precision of a few tenths of 1%. The integration procedure follows closely the "radial-tangential" scheme described by Smith (1978) and Gray (1976). In brief, we model the observed star as a rotating surface consisting of 1200 cells, 24 μ points (equal projected annulus areas), and 50 azimuthal points. For each cell, we assign a theoretical intensity profile based on the closest μ-value, and we compute the projected rotational velocity and a projected macroturbulent velocity. The macroturbulent velocities are generated using a so-called radial-tangential scheme, in which alternate cells carry radial or tangential velocity distributions, the actual velocities being computed from a Gaussian random-number generator. We use the same width parameter for both Gaussians. As in Paper I, each intensity profile is calculated assuming that the magnetic field vector is normal to the surface, as is usually the case for solar flux tubes. Thus, the global geometry of the fields is represented by a sprinkling of magnetic regions, uniformly scattered over the stellar surface, each vector being normal to the local surface. The specific dependence of magnetic effects on view angle is thereby accounted for fairly accurately.

Because the inherent model of turbulence in a disk integration scheme is quite different from that in simple Gaussian broadening, the characteristic values of turbulent velocity are different. Disk integrations generally require larger velocities to achieve the same effect on the profile. Furthermore, except in the instance of Fourier analysis of extremely high S/N line profiles (Gray 1976), it is difficult to distinguish the effects of rotational broadening from macroturbulence at the ± 1 km s^{-1} level. Errors of 1–2 km s^{-1} in the assumed value of rotation can be accommodated by choosing a different macroturbulent velocity, with errors in the resulting profile (owing to the intrinsic difference in the broadening functions) of about 0.3%. Thus, a literal interpretation of our broadening velocities (or anyone else's) is therefore not appropriate at moderate S/N ratios.

The other source of (nonmagnetic) line broadening is collisional broadening. As described in Paper I, we found we had to augment the Unsold (1955) C_6 parameter by factors of six and nine to match solar data for our lines. Other studies have yielded similar effects (e.g., Holweger 1972). We had to rederive the correction factors upon changing the *gf*-values. It became apparent during our analysis that with the new *gf*-values the solar data were no longer consistent with the old corrections (the required correction factors to C_6 became somewhat smaller) but that the K stars still demanded the old factors. We obtain these factors by fitting the lines (collision broadening affects the far wings while velocity broadening affects the core and near wings) for stars where magnetic fields are least likely to be present. The Sun is considered magnetic-free in our context and was used to set the correction in Paper I.

With the smaller corrections to C_6 now needed for the Sun, it became apparent that the resulting collisional broadening was insufficient in the synthesized profiles for the K stars. Because of the new *gf*-values we had to check the solar case with different iron abundances, and tried the Holweger (1972) solar model which is more appropriate for the more modern *gf*-values. This reduced—but did not eliminate—the apparent need for a correction C_6 that depended on spectral type. While less satisfactory than the situation in Paper I where a unique, solar-derived correction was used throughout, we are not overly disturbed by the spectral-type dependence. As with the velocity broadening, it may be that the true broadening mechanism is not fully treated here, and that the Unsold C_6 parameter contains an approximately correct relative dependence on density without actually encompassing all effects (as suggested by Dravins 1988, and by the need for large corrections in the first place!). It is also not clear to what extent errors in the model, or the use of single rather than multicomponent models, play a role. At any rate, we have continued to use a correction factor of 6 for $\lambda 8468$ and 9 for $\lambda 7748$ for the K dwarfs. An ex post facto justification is provided by the generally excellent fits our profiles have in the wings.

One issue which has concerned previous investigators is the influence of possible line blends in the wings of lines of interest. We dealt with this explicitly in Paper I, and outlined a modified χ^2 procedure which should reduce the effect of noticeable line blends (and noise spikes) on the derived "best-fit". We have implemented the ideas presented there in an objective procedure for choosing the best value for field strength and filling factor. We begin by calculating the composite profile for a given field strength and a set of filling factors by simply adding a null and magnetic profile together with the appropriate weightings. The error analysis is performed on the percentage difference profile between this calculated profile and the observed profile (which is interpolated onto the theoretical wavelength grid).

A threshold is chosen equal to several times the noise level, based on the variance of this difference vector in the continuum region. Any points in the difference profile which exceed this threshold are then set equal to it, to prevent undue weight being given to exceptional noise spikes or poorly treated line blends. This is because we expect that our calculated profile should fit an observed profile in its detailed shape, and that isolated regions of large discrepancies reflect problems outside the scope of the calculation. The "goodness of fit" is defined as the square root of the mean of the squares of the modified differences at each wavelength. The filling factor that yields the lowest value of this for each field strength is found, and the lowest of those for the range of field strengths tested becomes our derived stellar magnetic field. In almost all cases, a simple minimum is found at each strength for various filling factors, and similarly among various field strengths, so a more or less unique best-fit solution is evident. Examples of the difference vectors for three field strengths for ϵ Eri are shown in Figure 1. Note that any points which lie outside the chosen threshold line (2% for this case) are set equal to the threshold for the calculation of the "goodness of fit" statistic. This has a tendency to make all the poor fits have equally poor values, but they are always clearly much worse than the better fits.

The fields derived for stars in common with Paper I (using the same observations) differ somewhat from that work. This is due in part to the more objective procedure described above, but is primarily due to the change in *gf*-values for the two lines. The iron abundance and macroturbulent velocities have been rederived for the (now stronger) synthetic $\lambda 7748$ line. This adjustment does not have the same effect on synthetic $\lambda 8468$, since it is even stronger (relative to the old version). This means that some of the excess broadening in observed $\lambda 8468$ lines is made up by the increased oscillator strength. Thus, less magnetic field strength is required than in Paper I to provide the final needed increment of equivalent width, which appears largely in the wings.

Because our method computes the absolute equivalent width (as well as demanding a detailed match in the profile shape), the requirements on S/N and resolution may not be as stringent in deriving fields. If reasonably high quality echelle observations are employed which contain a large number of lines of different intrinsic strengths and magnetic sensitivities, one can, in principle, calculate the change in *equivalent width* that a given field will cause in all these lines compared to a magnetically null star with similar stellar properties. One may find a unique solution by demanding that all the lines change in the required fashion (depending on the *gf*- and Landé *g*-factor for each one. In essence, this compensates for the lack of precise profile information in a couple of lines with the many

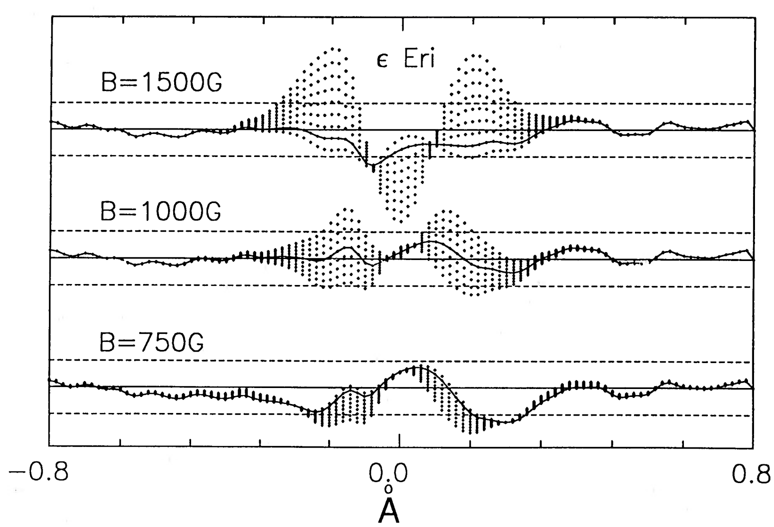

FIG. 1.—Ratios of observed $\lambda 8468$ profile to model profile for various assumed values of magnetic field strength, B, and filling factor. The three series of plots represent, from top to bottom, models constructed assuming $B = 1500$, 1000, and 750 G. Each series shows, for a particular value of B, the ratio of observed to model profile for a range of filling factors from 10% to 50%, in increments of 5%. The best fit (essentially minimum χ^2) in each series is denoted by a continuous line. Dashed lines show the $\pm 2\%$ levels. In this case, ϵ Eri, the best fit occurs for $B = 1000, f = 30\%$, with an rms of 0.006 of the continuum.

added constraints from a multiline analysis, while preserving the physical nature of the analysis. We are pursuing this possibility with Hamilton echelle spectra, the motivation being that one might be able to measure fields in substantially fainter stars, and with relaxed constraints on how slowly the star must be rotating to detect Zeeman effects.

III. OBSERVATIONS AND RESULTS

The Zeeman analysis described in Paper I, with modifications described in § II of this paper, has been applied to the sample of late G and early K stars shown in Table 1. The spectra were obtained on 1986 August 23 and 26 at the coudé focus of the 3 m telescope at Lick Observatory, with the same equipment as described in Paper I. Briefly, the grating VII and 80 inch (2 m) camera were used to yield a dispersion of ~ 0.034 Å pixel^{-1}. A slit width of 0".34 yielded instrumental profiles for $\lambda 8468$ and $\lambda 7748$, having widths of 66 mÅ and 74 mÅ, respectively, corresponding to ~ 2 pixels at the CCD. With exposures of 45–60 minutes, the S/N ratios obtained were between 100 and 200 for the program stars at $V = 6$. The rather long exposure times were due to vignetting and inefficiency of the grating, and to the narrow slit width. The spectra were reduced by standard techniques, and care was taken to ensure that zero-point errors were minimized. Several known blends reside in the red wings of both lines and were subtracted before analysis. For each star, the Zeeman insensitive flux profile, $\lambda 7748$, was synthesized and fitted to the observed profile using two free parameters, the iron abundance and the macroturbulent velocity. During this process, we fix the value of $v \sin i$, which is derived usually from Ca II rotation periods (Noyes *et al.* 1984), standard values of stellar radius, and from assuming $\langle \sin i \rangle = \pi/4$. The substantial uncertainties in $v \sin i$ are adequately masked by the choice of macroturbulent velocity, and the effects on both lines will be similar. The two free parameters, iron abundance and macroturbulent velocity, are nearly independent, as the first determines the equivalent width and the second effects the profile shape. Adopting these stellar parameters, the Zeeman-sensitive line, $\lambda 8468$, was then synthesized without any free parameters, under the assumption that the star had no magnetic field. For each star, a direct visual comparison was then made between the observed $\lambda 8468$ line and the synthesized profile. Special attention was given to the blue wing which suffers no appreciable blends.

Visual inspection of the profiles revealed two stars for which the observed and synthesized ($B = 0$) $\lambda 8468$ profiles were identical within photometric errors of 1% or less. Figure 2 shows the observed and synthesized $\lambda 8468$ profiles for these two apparently nonmagnetic stars, and one notices that neither of the observed profiles shows enhanced broadening in the core or the "shoulder." Indeed, the fits are quite satisfactory, considering that no free parameters were employed. However, we are disturbed that the very center of the observed line in σ Dra is brighter than that synthesized by 3%. This could be due to photon statistics in the core pixel or else to systematic effects outside our analysis (e.g., poor stellar model and/or bulk flows). It does appear that the observed profile of σ Dra is asymmetric in the entire core region. *We conclude that 54 Psc and σ Dra had no detectable magnetic field at the time of our observations.* We estimate that a magnetic field would have been detectable on either of these stars if the surface filling factor had been above $\sim 10\%$, for field strengths of about 1000 G. These are the only two stars in our sample which were clearly null results.

The same analysis on three other stars, HR 8832, 107 Psc, and HD 166620, revealed marginal evidence for Zeeman broadening. In these cases, the shoulders of the observed $\lambda 8468$ appear depressed on both the blue and red sides, indicative of Zeeman broadening. The amount of depression for all three stars is typically about 3%–5%, substantially greater than the 1% (or better) rms noise in the spectra. This depression is shown implicitly in Figure 3 at the bottom, where the differences (multiplied by 2) between the observed and synthesized ($B = 0$) profiles are shown as a dashed line, although the synthesized profile for $B = 0$ is not shown (for clarity). The difference profile for 107 Psc (*middle panel*, Fig. 3) shows the characteristic double-hump shape indicative of the presence of the underlying sigma components of the Zeeman triplet. In the case of HR 8832, the observed red and blue shoulders are also

TABLE 1

PROGRAM STARS: FINAL DERIVED STELLAR PARAMETERS

Star	B (G)	f (%)	Fe/H ($\times 10^{-5}$)	V_{macro} (km s^{-1})	$v \sin i$ (km s^{-1})
ξ Boo A	1600	22	2.15	3.55	2.5
ϵ Eri	1000	30	2.8	3.0	1.0
61 Cyg A	1200	24	1.9	1.7	1.0
70 Oph A	1200	18	3.6	2.1	2.5
36 Oph A	1500	13	2.8	2.4	1.6
HR 222	1600	12	2.1	2.1	0.7
HR 8832	1000:	17:	4.55	1.8	1.0
107 Psc	1000:	17:	3.15	2.0	0.7
HD 166620	1500:	11:	1.6	2.6	0.8
σ Dra	...	...	2.0	2.1	1.0
54 Psc	...	...	4.7	1.8	0.9

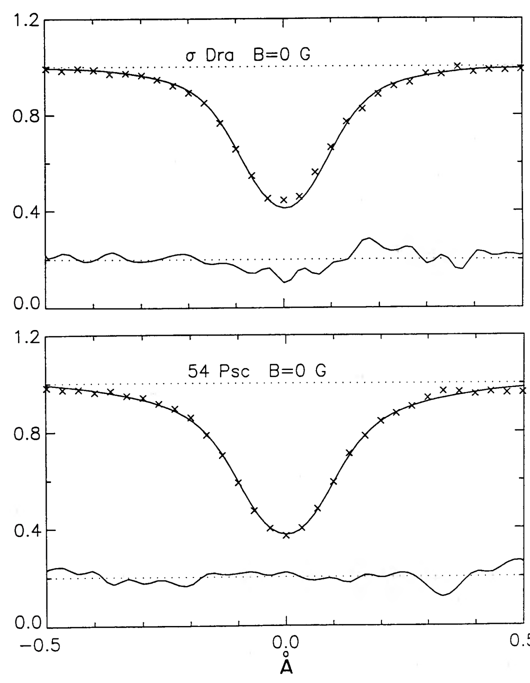

FIG. 2.—The nondetections of Zeeman broadening. The panels show the observed profile (*crosses*) and the model profile, constructed for $B = 0$ (*dotted line*) for $\lambda 8468$. Note that the matches are good, indicating no apparent Zeeman broadening of the observed profile. At bottom is shown the difference, multiplied by 2. The noise ($\sim 1\%$) in the observed profile is apparent by inspection of the far wings.

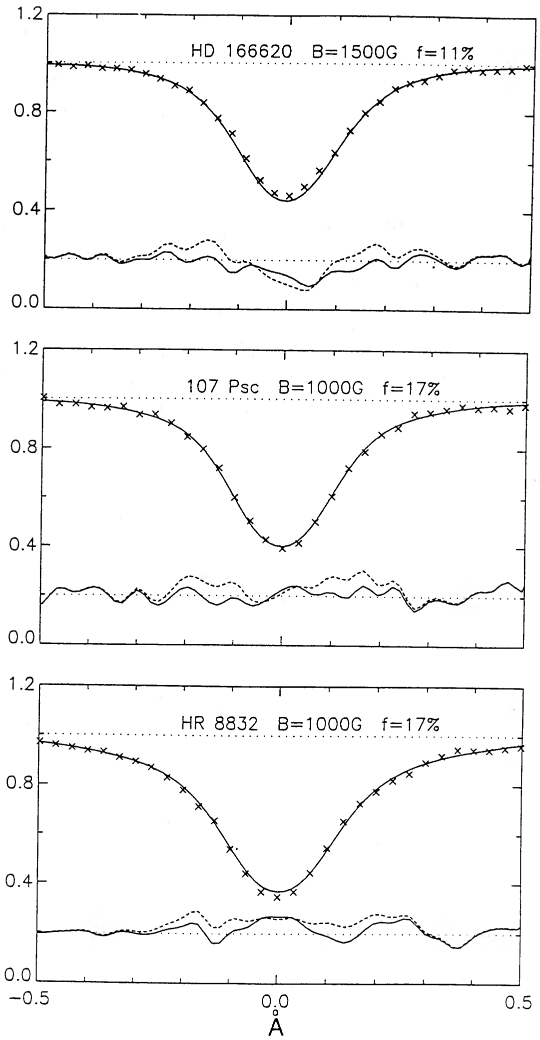

FIG. 3.—The marginal detections of Zeeman broadening. The panels show the observed profile (*crosses*) and the best-fit model profile (*dotted line*) constructed with a magnetic field strength, B, and filling factor, f, given at top. The fits are good in each case, especially in the wings where the Zeeman effect is greatest. At the bottom of each panel is shown the difference (multiplied by 2) between observed and best-fit profile (*solid line*) and the difference between observed and $B = 0$ model profile (*dashed line*). Note that the $B = 0$ difference profiles (*dashed line*) show only marginal evidence for the characteristic "double-hump" pattern, indicative of Zeeman broadening.

depressed, but so is the core (an effect we do not understand). Note that we cannot "fix" this by changing parameters because of the excellent fit (not shown) for our Zeeman-insensitive (λ7748) line, and the fact that we have no free parameters in fitting λ8468.

For the above three marginal detections we have proceeded to synthesize the observed profile by including magnetic fields as described in § II. The synthesized profiles that best fit the observed λ8468 for each of the stars are shown in Figure 3 (*solid line*). The fits are satisfactory in each case, with discrepancies being consistent with errors in photon statistics. Note, however, that the cores of HD 166620 and HR 8832 are not fit well, an effect which should be confirmed with improved observations. On the other hand, the occasional profile discrepancies found may be indicative of systematic errors. Our work in progress on the inclusion of flux-tube models for the magnetic regions suggests that the simple one-component atmospheres used here can cause such profile discrepancies. In any case, it is clear that the inclusion of magnetic fields in the line synthesis has significantly improved the fit to the observed profile. The differences (multiplied by 2) between the observed and best-fit synthesized profiles are displayed at the bottom of each panel in Figure 3 with a solid line. In all cases there is an apparent reduction of the differences when a field is included compared to the no-field trial; however, it is obvious that the accuracy of these determinations is poor. The final magnetic field strengths and filling factors are given in Table 1.

The six remaining stars in our sample, ϵ Eri, ξ Boo A, 70 Oph A, 36 Oph A, HR 222, and 61 Cyg A, all showed marked depression of the shoulders of the observed λ8468 relative to the synthesized profile constructed with no field. In all cases the fits to the Zeeman insensitive profile λ7748 were good. Thus, for these stars, the evidence is strong for the presence of magnetic fields. Figure 4 shows the differences (multiplied by 2) between the observed and synthesized ($B = 0$) profiles with the dashes at the bottom. In each case, the characteristic double-hump pattern is clearly visible, suggesting Zeeman broadening. Models were run for each star with magnetic fields included until a best fit was achieved. The resulting best-fit synthetic profiles are also shown overlaid in Figure 4 (*solid line*).

In each of these six cases of clear Zeeman broadening, the fits of the synthetic profile are excellent and completely consistent with the known photometric errors. Indeed, we found no difficulties in modeling either the Zeeman-sensitive or Zeeman-insensitive lines for these six stars. One might expect that the recognition of a Zeeman broadening in λ8468 would require that the Zeeman-insensitive line λ7748 be synthesized anew, yielding perhaps a different iron abundance and macroturbulence. However, only in ξ Boo A does the inclusion of a magnetic field (as measured) significantly change the synthetic λ7748 profile, and then only marginally. This is because of the small Landé g-factor for λ7748, confirming its usefullness as a "null" line. The magnetic field strengths and filling factors for these six stars (along with the other program stars) are given in Table 1, along with the $v \sin i$ used and the derived values of macroturbulence and iron abundance. In summary, the field strengths range from 1000 to 1600 G and the filling factors range from 12% to 30%. We note again that the values given here for ϵ Eri, ξ Boo A, and HD 166620 are slightly different from those given in Paper I owing to the refinements in gf-values and the use of disk integration here.

We note that the observed lines appear symmetric at the 1% level, indicating that blends have been adequately removed by our procedure and that bulk flows are not a major factor. We have actively searched for other explanations of the excess broadening of the λ8468 line other than the Zeeman effect. We explored modified turbulence, gf-values, stellar rotation, and atmospheric depth structure. None was found to explain the excess broadening. Thus we conclude that the detections and analysis of Zeeman broadening made here represent compelling evidence of kilogauss fields on late-type stars.

IV. DISCUSSION

a) Integrity of the Magnetic Measurements and Comparison with Other Studies

We consider now the issue of the reliability of the detections and measurements of magnetic fields derived by our approach.

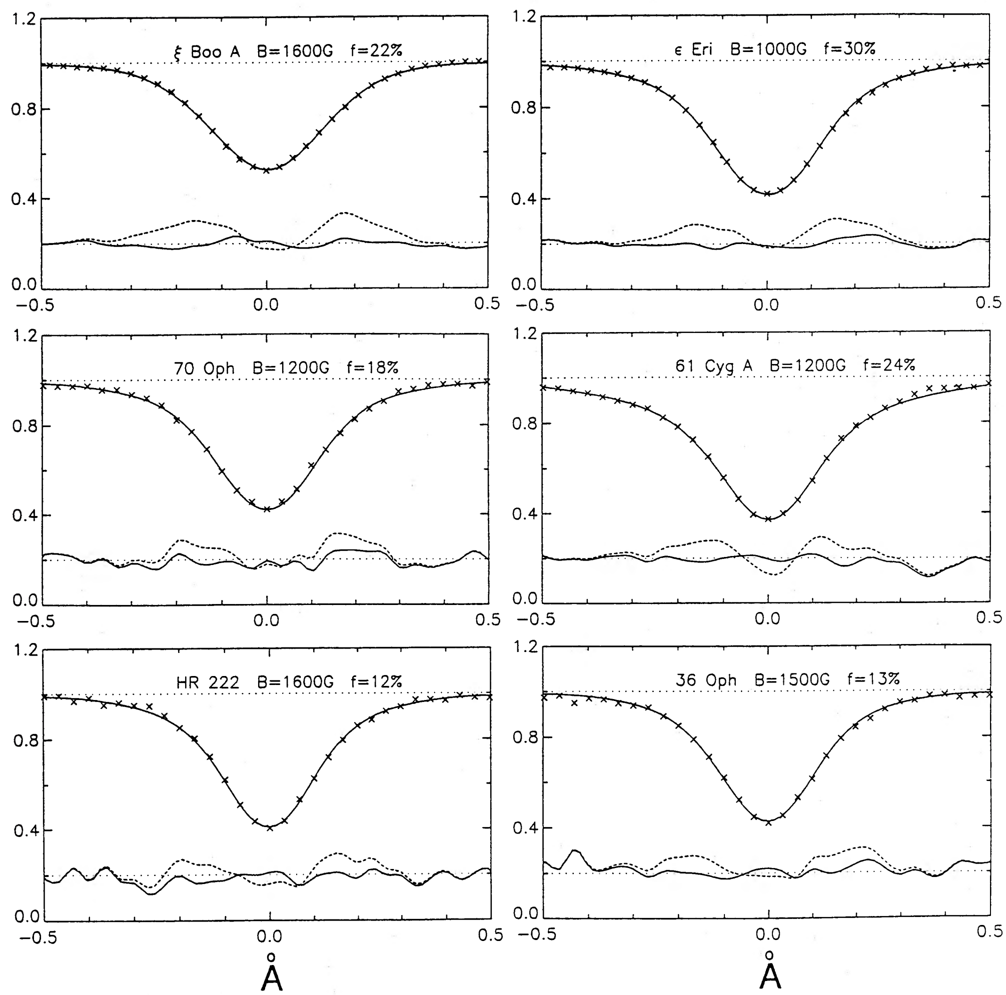

FIG. 4.—Clear detections of Zeeman broadening for six stars. Each panel contains the same information as in Fig. 3. Note the clear "double-hump" pattern of the difference between the observed and $B = 0$ model profile (*dashed line, at bottom*).

One measure of reliability may be derived from the quality of the theoretical fits to the observed λ8468 line. Since there are *no free parameters in the synthesis of the λ8468 line*, inadequacies in the theory may show up as discrepancies between observed and synthetic profiles. Figure 4 shows these discrepancies at the bottom of each panel for two synthetic models, one constructed without an assumed magnetic field, and the other with one. It is clear that without an assumed field, the differences are typically much larger than the photometric errors of 1% or less. *Thus, LTE model profiles constructed without magnetic fields simply do not reproduce observed profiles.* At the same time, for synthetic profiles constructed with an assumed magnetic field, the differences between theoretical and observed profiles (also shown at bottom of Fig. 4) are typically consistent with the 1% photometric errors. Even in the most magnetic stars such as ε Eri and ξ Boo A, the differences between theory and observation are very small, although the only free parameter in the synthesis is the magnetic field. We regard the good quality of the fits as strong evidence that the line synthesis satisfactorily contains the relevant physics.

On the other hand, the errors in these magnetic field measurements must be substantial. The magnitude of the depression of the line wings due to the Zeeman effect in even the most magnetic stars is evidently ~5%, as shown in the difference profiles, so the photometric errors of typically 1%–$\frac{1}{2}$% imply that the magnetic field measurements have an effective S/N ratio of only 5–10. Of course, ~12 points in the flux profile are used in the fit, so the precision may be somewhat better. We expect that the magnetic field measurements must carry random errors of ~20%. Saar (1988*a*) has discussed errors in Zeeman broadening measurements in detail. The noise in the spectra not only limits the precision of B and f, but also inhibits the unique separation of the two (Saar 1988*a*). Several authors have noted that the quantity $B\sqrt{f}$ is more precise than either B or f separately (Gray 1984; Saar 1988*a*), and the random errors in the present Zeeman broadening measurements must behave similarly.

Ideally, the integrity of the present measurements could be assessed by comparison with other such measurements, such as those of Marcy (1984), Gray (1984), Saar (1988*b*), and Mathys and Solanki (1988). Unfortunately, the possible time variability of the fields may prevent useful comparison, and, more importantly, all past approaches are sufficiently divorced from physical rigor that systematic differences probably dominate. The best "standard" star for intercomparison of the various techniques is probably ε Eri since all groups have observed it and there is near consensus that Zeeman broadening is present. The reported field strengths and filling factors are, in order of authors given above, (1170 G, 67%), (1900 G, 30%), (1900 G, 11%), and (2090–2960 G, 30%–45%), to be compared with our measurement, (1000 G, 30%). Saar (1988*a*) also obtained a high-quality FTS infrared spectrum showing no Zeeman splitting at all, although splitting is seen in sunspots.

We have reanalyzed Saar's (1988*a*) infrared spectrum using our line synthesis technique. In particular, we have synthesized the Na I line at 2.209 μm (Landé $g = 1.33$) for several assumed values of magnetic field strength and filling factor. Unfortunately, a precise oscillator strength is unavailable for this line, so we adopted a value for gf that yielded an equivalent width nearly equal to that observed. As usual, intensity profiles were generated for eight μ points on the stellar surface, and a disk integration was done using the same values for $v \sin i$ and macroturbulent velocity that were used in the synthesis of λ8468. As a test, we tried the case, $B = 2900$ G, $f = 100\%$, to synthesize Saar's observed sunspot profile, and immediately obtained a Zeeman-split synthetic profile that was quite similar to that observed.

Representative 2.2 μm results for ϵ Eri are shown in Figure 5 for the four cases: ($B = 0$), (1000 G, 30%), (3000 G, 8%), and (2400 G, 30%). The latter two cases are representative of magnetic values derived by Saar (1988*a*) and Mathys and Solanki (1988). In each case, the synthesized profile (*solid line*) is laid over Saar's observed profile (*crosses*). One notices that the synthetic profile for $B = 2400$, $f = 35\%$ (*bottom*) has significantly stronger wings than the observed profile. This shows clearly that if the true field strength on ϵ Eri is near 2400 G or higher, the filling factor was substantially less than 30% at the time of observation. The synthetic profile for $B = 3000$ G, $f = 8\%$ fits the observed profile marginally well, although the shortward wing is not fitted well, apparently due to an asymmetry in the observed profile. The discrepancy in the core is due to the fact that the observed profile is slightly shallower than is possible with *any* LTE line in our scaled solar model at this wavelength. Clearly, however, filling factors larger than $\sim 10\%$ are ruled out for $B = 3000$ G. The synthetic profile for $B = 1000$ and $f = 30\%$ fits reasonably well, especially considering that the oscillator strength is so poorly known, and that the observed profile has that asymmetry of unknown origin. Finally, the synthetic profile for $B = 0$ also fits reasonably well, within the uncertainties here, so that we cannot rule out the possibility that there is no field on ϵ Eri, based on these infrared data. The problem is that the advantage of using longer wavelengths has been largely mitigated by the lower magnetic sensitivity of this line compared to λ8468. In summary, this 2.2 μm analysis enables us to rule out high field strengths at high filling factors at the time of the FTS measurement. We note that the measurement by Mathys and Solanki (1988) mentioned above is considerably higher than this limit, implying either large field changes on ϵ Eri, or errors in the Zeeman analysis.

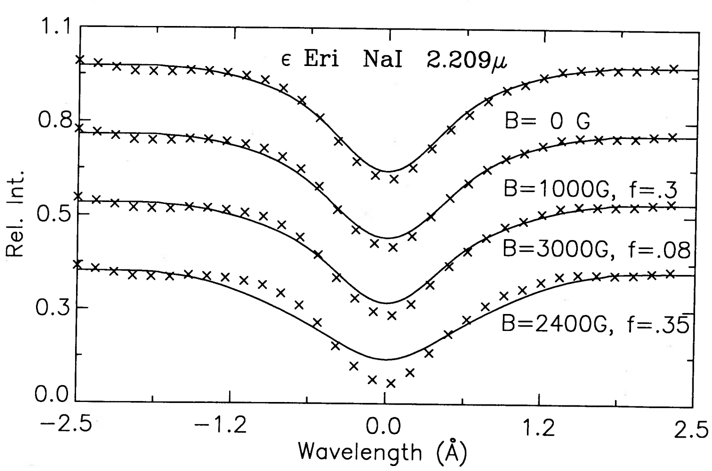

FIG. 5.—Zeeman analysis of infrared spectrum of ϵ Eri. The observed Na I 2.2 μm line (*crosses*) and model profiles (*solid line*) are shown for various assumed values of B and f. Note that high field strengths ($B > 2400$ G) and high filling factors yield unacceptable fits. The observed profile is from Saar (1988*a*).

Another source of uncertainty in the Zeeman measurements derives from the unknown distribution of fields over the stellar surface. For example, a spatial concentration of fields on the limb will result in a Doppler-shifted Zeeman pattern, removing the symmetry in the observed flux profile. Saar (1988*a*) has estimated these effects to be small in the deduced field strength, but occasionally large in the deduced filling factor, for extreme distributions. Another source of error derives from uncertainties in the gf-values of the lines. In changing from Kurucz and Peytremann's values to those of Blackwell's group, the deduced magnetic field strengths and filling factors for ϵ Eri changed insignificantly. However, for ξ Boo A, the values changed from (1200 G, 40%) to (1600 G, 22%). If Blackwell's gf-values are still in error by as much as the differences between the two sets of values, then the above test represents estimates of the resulting errors in the magnetic field.

b) *Correlations with Other Stellar Quantities*

It should be obvious from the section above that better observations and a more exhaustively tested Zeeman analysis will be required before high confidence can be placed on relations between measured stellar magnetic fields and other stellar parameters. The primary intent of this series of papers is to refine our ability to analyze the Zeeman effect in line profiles of cool stars. Nonetheless, it is worthwhile at this juncture to take a peek at possible relations that might be emerging. We note that a much more extensive observational set has been studied by Saar (1987), although not with our physical analysis.

We consider here the possible relationship between the magnetic field measurements and two stellar observables, namely, chromospheric Ca II, H, and K emission and rotation period. Rotation periods were taken from Vaughan *et al.* (1981) and Noyes *et al.* (1984) and the HK index R'(HK) was taken from Noyes *et al.* (1984). To represent each star's magnetic field, we chose the product of field strength and surface filling factor, Bf, both because it is a physically meaningful quantity (surface-averaged magnetic flux per unit area), and because it is relatively precise compared with B or f separately.

A plot of R'(HK) versus Bf is presented in Figure 6 and shows a definite positive correlation of Ca II emission with magnetic field. The most discrepant point, located near the lower right corner is 61 Cyg A, a star which is much cooler than the other stars in this study, and perhaps should not be included at all ($T_{\rm eff} = 4300$ K, while all other stars have $T_{\rm eff} > 5000$ K). Nonetheless, Figure 6 shows that the stars with the strongest chromospheres have the largest values of Bf, and the two stars that exhibited no Zeeman broadening (upper limits shown) are among those with the weakest chromospheres.

An analysis of Bf versus rotation period also shows a definite correlation in the sense that fast rotators have larger values of Bf. Closer inspection suggests that the residuals are correlated

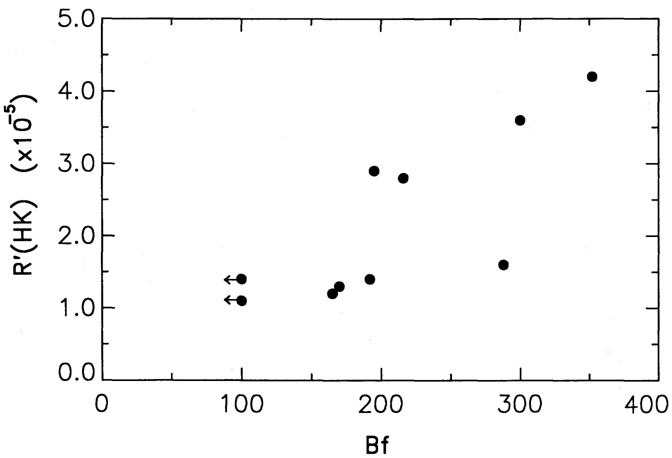

FIG. 6.—Chromospheric Ca II H and K index, R'(HK), vs. Bf

with effective temperature, i.e., stellar mass. Indeed, inclusion of a power-law dependence on $T_{\rm eff}$ as a second independent parameter yields significantly tighter correlation. Figure 7 shows the measured Bf versus $P_{\rm rot}\,T_{\rm eff}^4$ in which a good correlation is apparent.

We find that in general the quantity $P_{\rm rot}\,T_{\rm eff}^n$, for positive values of n, correlates better with Bf than does $P_{\rm rot}$ alone. Negative values of n yield very large scatter and are ruled out. We feel that a formal multivariate fit to determine power-law exponents is unwarranted at this time owing to the possible systematic and considerable random errors (~20%) in Bf. However, the measurements suggest that magnetic fields on G and K dwarfs increase not only with rotation rate, but also with decreasing stellar mass. This dependence on stellar mass is not convincing because of the small range in stellar masses represented, with only 61 Cyg A being considerably different in mass. This result, however, is reminiscent of the observed higher prevalence of magnetic fields on K dwarfs compared with G dwarfs (Marcy 1984; Gray 1984; Saar 1988*b*). The stellar mass dependence is also qualitatively consistent with

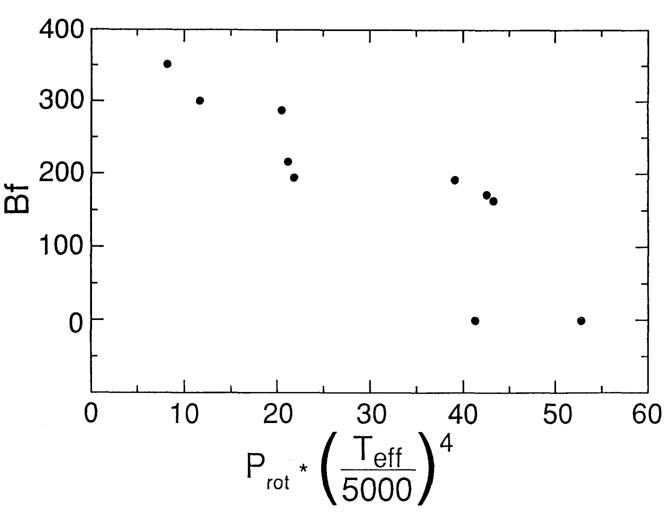

FIG. 7.—Product of field strength and filling factor, Bf vs. $P_{\rm rot}\,T_{\rm eff}^4$. The correlation suggests that Bf increases with stellar angular velocity and decreases with stellar mass. The exponent of "4" for $T_{\rm eff}$ is suggestive only, as other similar positive integers also yield acceptable correlations.

the notion that Rossby number plays a role in determining surface magnetic fields, as the convective turnover time is thought to increase with declining stellar mass on the main sequence (e.g., Gilliland 1985; Noyes *et al.* 1984). We do not feel justified in going beyond these brief and qualitative remarks until the systematic and observational errors are further reduced and the observational sample is expanded.

V. SUMMARY AND CONCLUSIONS

The Zeeman analysis employed here is distinguished from past efforts in that it is closely tied to the actual physical processes that produce Zeeman-broadened absorption lines in G and K stars. The radiative line transfer in all Stokes parameters is computed for a model stellar atmosphere, and the resulting intensity profiles are disk-integrated to model the stellar rotation and macroturbulence. The observed and synthetic Zeeman-insensitive line, λ7748, is used to fix the iron abundance and the macroturbulence, permitting construction of the Zeeman-sensitive line, λ8468, with *no free parameters* in the absence of a magnetic field. Zeeman broadening is then detected as an excess broadening, especially in the wings, between the synthesized λ8468 profile and the observed profile. The actual field strength is deduced by constructing trial synthetic λ8468 profiles for various assumed magnetic field strengths and surface filling factors, and searching for a best fit to the observed profile.

We have observed a sample of 11 G8–K5 main-sequence stars with high resolution and S/N ratio. Two stars (σ Dra and 54 Psc) were found to exhibit no Zeeman broadening at all, thereby establishing convincingly that magnetically weak K stars do exist. In addition, three stars had sufficiently little Zeeman broadening that only a marginal detection could be assigned. The remaining six stars showed clear Zeeman broadening, with field strengths in the range 1000–1600 G, and surface filling factors up to 30%.

The product of field strength and filling factor, Bf, correlates with both chromospheric Ca II emission and with stellar rotation, in the sense that stars with substantial magnetic fields have strong chromospheres and short rotation periods. We find that the value of Bf correlates best with the quantity $P_{\rm rot}\,T_{\rm eff}^n$ where n is positive, although a better determination of n is not possible with current measurements. From the standpoint of dynamo theory, this suggests that surface magnetic fields increase not only with stellar angular velocity, but also, with decreasing stellar mass. This result is in qualitative agreement with the notion that the Rossby number governs the production of magnetic fields. While the ultimate scientific payoff is related to these issues, the current work concentrates primarily on the developing Zeeman analysis. Once this is settled, extensive further observations will be needed to make progress on the stellar physics.

Somewhat puzzling is the relatively strong magnetic field for 61 Cyg A, a chromospherically inactive star, based on a variety of diagnostics (e.g., Noyes *et al.* 1984; Simon and Fekel 1987). The nondetection of Zeeman *splitting* in infrared FTS spectra of 61 Cyg A by Saar and Linsky (1985) may be nonetheless consistent with a modest field strength near 1000 G and a modest surface covering factor. Further, the chromospheric emission in the Ca II H and K lines are known to vary by a factor of 2 (Wilson 1978) over time scales of years and even days. In this regard, Figure 6 suggests that the quantity Bf for 61 Cyg A was ~2 times its expected value given its average value of R'(HK). Assuming the field strength does not vary from its measured value of 1200 G, one might infer that the filling factor was, at the time of observation, ~ 2 times its average value. Thus, this change in filling factor would not be inconsistent with the known variations of chromospheric H and K emission. Clearly, future efforts should be made to obtain simultaneous measurements for this star. Alternatively, the relation between *Bf* and *R*′(HK) might be a function of spectral type, as hinted above. A Zeeman technique that works reliably for fainter stars is needed to solve this problem.

Finally, we suspect that the largest source of uncertainty in these magnetic field measurements is due to the simplified one-component atmosphere employed. As on the Sun, the magnetic regions on other stars must be located in regions having different atmospheres than in the nonmagnetic regions. The mechanical heating and evacuation of these "stellar faculae" imply that the present line transfer calculations, which assume a scaled "quiet" photosphere everywhere, can be improved. Thus there is considerable need for two-component modeling of both photometric and spectroscopic data of active stars to learn about the characteristics of the stellar faculae.

We would like to acknowledge helpful conversations with S. Saar and L. Hartmann. This work was supported in part by NSF grants AST 86-03979 to G. W. M. and AST 86-16863 to G. B. Observations at Lick Observatory are supported in part by NSF block grant AST 86-14510 to the University of California.

REFERENCES

Basri, G., and Marcy, G. 1988, *Ap. J.*, **330**, 274.
Blackwell, D. E., Petford, A. D., Shallis, M. J., and Simmons, G. J. 1982, *M.N.R.A.S.*, **199**, 43.
Bruning, D. H. 1984, *Ap. J.*, **281**, 830.
Dravins, D. 1988, in *IAU Symposium 132, The Impact of Very High S/N Spectroscopy on Stellar Physics*, ed. Cayrel de Strobel and M. Spite (Dordrecht: Kluwer), p. 239.
Gilliland, R. L. 1985, *Ap. J.*, **300**, 339.
Gray, D. F. 1976, *The Observation and Analysis of Stellar Photospheres* (New York: Wiley), p. 426.
———. 1984, *Ap. J.*, **277**, 640.
Holweger, H. 1972, *Solar Phys.*, **25**, 14.
Kurucz, R. L., and Peytremann, E. 1975, *A Table of gf Values, Smithsonian Ap. Obs. Spec. Rept.*, No. 362.
Marcy, G. W. 1984, *Ap. J.*, **276**, 286.
Mathys, G., and Solaniki, S. K. 1988, preprint.
Noyes, R. W., Hartmann, L. W., Baliunas, S. L., Duncan, D. K., and Vaughan, A. H. 1984, *Ap. J.*, **279**, 763.
Robinson, R. D., Worden, S. P., and Harvey, J. W. 1980, *Ap. J. (Letters)*, **236**, L155.
Saar, S. 1987, Ph.D. thesis, University of Colorado.
———. 1988*a*, *Ap. J.*, **324**, 441.
———. 1988*b*, in *IAU Symposium 132, The Impact of Very High S/N Spectroscopy on Stellar Physics*, ed. Cayrel de Strobel and M. Spite (Dordrecht: Kluwer), p. 295.
Saar, S., and Linsky, J. L. 1985, *Ap. J. (Letters)*, **299**, L47.
Simon, T., and Fekel, F. C. 1987, *Ap. J.*, **316**, 434.
Smith, M. A. 1978, *Ap. J.*, **224**, 584.
Unsold, A. 1955, *Physik der Sternatmospharen* (2d ed.; Berlin: Springer), p. 326.
Vaughan, A. H., Baliunas, S. L., Middelkoop, F., Hartmann, L. W., Mihalis, D., Noyes, R. W., and Preston, G. W. 1981, *Ap. J.*, **250**, 276.
Wilson, O. C. 1978, *Ap. J.*, **226**, 379.
Unno, W. 1956, *Pub. Astr. Soc. Japan*, **8**, 108.

GIBOR BASRI: Department of Astronomy, University of California, Berkeley, Berkeley, CA 94720

GEOFFREY W. MARCY: Department of Physics and Astronomy, San Francisco State University, San Francisco, CA 94132